

19. PROBABILISTIC MODELING OF TORNADO PATH LENGTH INTENSITY VARIATION USING F/EF-SCALE DAMAGE DATA

Melissa K. Faletra*, Lawrence A. Twisdale, and Sudhan S. Banik

Applied Research Associates, Inc., Raleigh, NC

ABSTRACT

The intensity of a tornado varies over its life cycle and generally includes a formation stage, a mature stage and a dissipation stage. Tornadoes do not typically exhibit their maximum intensity over their entire recorded path length. As a result, modeling and analysis of tornado path length intensity variation (PLIV) is an important part of tornado wind speed risk analysis.

In support of the National Institute of Standards and Technology's (NIST) project to create tornado risk maps for building design, a probabilistic model of tornado path length intensity variation (PLIV) was developed from tornado damage data. The data sources used for PLIV modeling consist of both non-geo-referenced and geo-referenced damage maps. For the non-geo-referenced map analysis, historically mapped tornadoes were used to create catalogs of F/EF scale ratings in the PLIV sequence that they occur (along with each rating's appropriate length portion). The geo-referenced PLIV analysis was based on the NWS Damage Assessment Toolkit (DAT) data for the years 2008-2015. Damage indicator data and contour data from the DAT were both examined, and individual event PLIV catalogues were also developed for this dataset.

The paper presents PLIV analysis results and discusses needs for improved data collection to support PLIV modeling. The paper concludes with PLIV data converted to wind speeds and illustrates spline fits of example PLIV catalogues in which the EF scale intensity ratings have been converted to wind speeds. An advantage of this modeling process is that it separates the analysis of damage intensity variation along a tornado path length from the estimation of wind speeds given a damage rating.

1. INTRODUCTION

Tornadoes do not usually exhibit their maximum intensity over their entire recorded path length. Radar data shows that intensity can both persist as well as change rapidly along the tornado path, e.g. Kosiba et al. (2013) and Burgess et al. (2002). While radar observations provide direct estimates of tornado wind speeds, sufficient radar data does not exist to probabilistically analyze intensity variation along complete tornado path lengths. Detailed damage maps in highly developed areas often demonstrate that tornadoes are capable of maintaining high intensity for relatively long distances. For examples see the 2013 Moore, OK tornado (Atkins et al., 2014), the Joplin, MO tornado of 2011 (Marshall et al., 2012), the Greensburg, KS tornado of 2007 (Marshall et al., 2008a), and the Parkersburg, IA tornado of May 25, 2008 (Marshall et al., 2008b) maps. While many tornadoes are capable of persistent intensity, non-supercell tornadoes are also likely to be brief and less intense (Wakimoto and Wilson, 1989).

Tornado wind speed risk is related to the wind speed swaths (footprints) produced over the ground by a

tornado.¹ Since damage observations are the basis for classifying tornado intensities (from which wind speeds can be estimated), an approximate measure of a tornado's intensity variation during its life cycle can be obtained by analyzing F/EF scale rating variations along the length of the tornado's path.

We refer to the maximum intensity variation along a tornado's reported path length as path length intensity variation (PLIV). PLIV is based on the maximum intensity observed along the path length at various stages in the tornado's life cycle. PLIV does not consider wind speed deviations from the maximum intensity across the path width. We believe these deviations are best handled with a tornado windfield model. A probabilistic tornado windfield model (Twisdale, 1983) provides for detailed analysis of local windspeed variations, including the tornado wind characteristics across the path width. This approach has the advantage of producing tornado wind speed time-histories (for modeling loads on buildings) and swaths (for windspeed frequency analysis) that also incorporate tornado life cycle intensity variation.

The methods used herein to model PLIV capture the macro-scale changes in tornado intensity, providing intensity estimates over intervals of tornado path length.

* *Corresponding author address:* Melissa K. Faletra, Applied Research Associates, Inc., 8537 Six Forks Rd., Suite 600, Raleigh, NC 27615; e-mail: mfalet@ara.com

¹ Each point in the swath represents the maximum wind speed experienced at that location from the translating tornado.

Within this context, radar observations over a portion of a path length provide micro-scale level information on intensity variations.

The first attempt to model PLIV for tornado risk analysis was developed by Twisdale et al. (1978, 1978a). This analysis used Fujita's damage assessment and mapping of 148 tornadoes in the April 3-4, 1974 outbreak (Fujita, 1975). Fujita's team flew every tornado path and produced a map where they rated the maximum F-Scales along each path length at an average of 4 mile intervals over all the tornado paths (see Figure 1). This approach produced a systematic source of data on which to estimate PLIV.

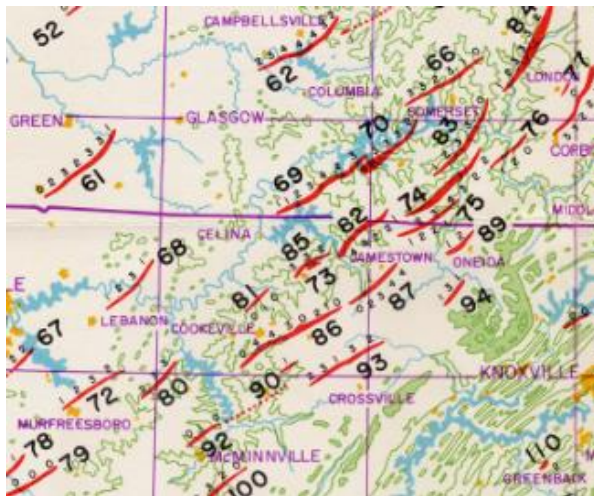


Figure 1. Portion of Non-Geo-Referenced Map of April 3-4, 1974 Super Tornado Outbreak (Fujita, 1975)

In 1981, Twisdale et al. (1981) expanded the analysis to include additional tornadoes, using data from the Red River Valley tornado outbreak of April 10, 1979 (Fujita and Wakimoto, 1979), the Bossier City, Louisiana tornadoes (Fujita, 1979), the Grand Gulf, Mississippi tornadoes (Fujita, 1978), and the Cabot, Arkansas tornado (Forbes, 1978) to supplement the April 3-4, 1974 outbreak. For these 150 ≥F1 tornadoes, the path lengths of each local F-Scale rating, within each tornado F-Scale rating, were summed and divided by the total length of all tornadoes in the tornado F-Scale rating, calculating the mean fraction of each local F-Scale intensity (I^*) within each tornado F-Scale rating (see Twisdale (1978) for the analysis details). The result ($P(I^*|F)$) was a tornado intensity variation matrix of conditional probabilities of local path intensity along the entire path length, given the rated tornado intensity (F). These conditional probabilities can be thought of as “mean fractions” of the path length for each intensity \leq the maximum intensity. Table 1 shows these mean fractions from the 1981 analysis. For example, a F5

tornado has F5 intensity over 15% of its path length, and a F4 tornado has F4 intensity over 21% of its path length. The importance of PLIV is therefore significant in tornado risk analysis. If one were to assume that a F5 tornado maintained F5 intensity over its entire path length, then the F5 risk would be about 6.7 (1/0.149) times larger than what one would estimate based on Table 1. An interesting observation from Table 1 is that the principal diagonal ($P(I^*|F = I^*)$, highlighted in red) shows a steady decrease in the fraction of length that a tornado was rated at its maximum intensity as the F-scale rating increases.

The data in Table 1 suffers from the well-known limitations of damage based intensity ratings, including the potential for an error of at least ± 1 F-Scale rating and limited damage information due to the spacing of available damage indicators (DIs) (see Twisdale et al. (2016) for a discussion of damage-to-wind-speed uncertainties and limitations). Nevertheless, when coupled with probabilistic modeling and tornado windfield modeling (for path width wind speed variation), the PLIV data provides a key element in tornado wind speed risk analysis.

Table 1. Mean Fraction Table: $P(I^*|F)$ from Twisdale et al. (1981)

| Local PL Intensity | Tornado Rating | | | | | |
|-----------------------|----------------|-------|-------|-------|-------|-------|
| | ≤F0 | F1 | F2 | F3 | F4 | F5 |
| ≤10* | 1.00 | 0.572 | 0.280 | 0.116 | 0.142 | 0.133 |
| 11* | | 0.428 | 0.352 | 0.245 | 0.158 | 0.102 |
| 12* | | | 0.368 | 0.318 | 0.278 | 0.189 |
| 13* | | | | 0.321 | 0.210 | 0.242 |
| 14* | | | | | 0.212 | 0.185 |
| 15* | | | | | | 0.149 |
| No. Tors = 150 | | 34 | 40 | 41 | 29 | 6 |

We note that a similar approach and data were adapted by others for simplified tornado risk assessment approaches, such as Reinhold and Ellingwood (1982), and Ramsdell and Rishel (2007). However, these papers used damage ratings to infer intensity across the path width in order to produce empirical estimates of damage areas by F/EF scale. The PLIV approach herein is limited to macro-level intensity variation of the tornado along the path length, since a tornado windfield model is used for path width wind speed variation and to produce tornado wind speed swaths.

Tornado life cycle intensity variation along the path length is an important element in tornado risk modeling for engineering analysis and design. As pointed out by Edwards et al. (2013), damage-based tornado intensity ratings are expected to have an important and continued role in the long-term risk assessment of tornadoes.

The goal of this paper is to update the analysis of PLIV with a re-evaluation of the pre-1981 data and new data since 1981. We begin in Section 2 with an updated analysis of the non-georeferenced (NGR) damage map data. The NGR analysis is followed by a review of the DAT in Section 3 and an analysis of georeferenced (GR) EF DAT data (NOAA, 2016) (see Figure 2) in Section 4. In both NGR and GR analyses, we create catalogs of the PLIV damage data. A “catalog” refers to a record of F/EF scale ratings for an individual tornado, in the PLIV sequence that they occur along the tornado path, in addition to each rating’s corresponding length portion. Catalogs are developed from tornado damage maps for 155 NGR tornadoes and 734 geo-referenced tornadoes. We conclude with comparisons of the results in Section 5 and present catalogues of the NGR PLIV data in Section 6.

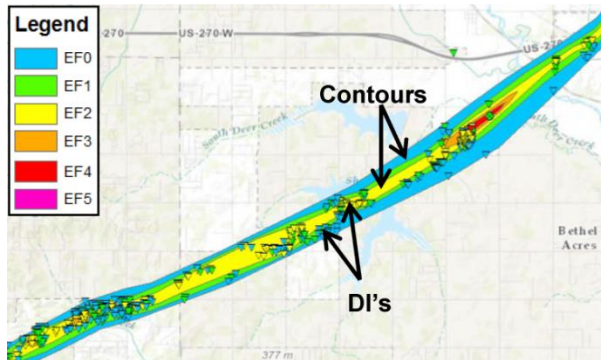


Figure 2. Example of Geo-Referenced Damage Data: Data from NWS DAT (NOAA, 2016).

2. NON-GEO-REFERENCED PLIV DATA

NGR data was analyzed and PLIV catalogs were created for the data. The catalogs were produced for NGR data from the original data in the Twisdale et al. (1981) model that we were able to get individual ratings along the path from (April 3-4, 1974 and Red River Valley tornadoes), as well as from newer, NGR PLIV data from subsequent surveys following the 1981 research. All of the NGR data used in this study is summarized in Table 2. The data from Twisdale et al. (1981) with individual ratings along the path, combined with the more recent NGR tornadoes, amounted to 176 historically mapped tornadoes with PLIV information. PLIV catalogs were created manually for these 176 NGR tornadoes, assuming equal segment lengths for each rating within a tornado.

Table 2. Post 1981 Research NGR PLIV Data

| Event | Source | Date | No. Tors. | | | | | |
|---------------------------------------|--------------------------|----------|-----------|-----------|-----------|-----------|-----------|-----------|
| | | | F0 | F1 | F2 | F3 | F4 | F5 |
| Pre-1981 NGR Data | | | | | | | | |
| Red River Valley | Fujita & Wakimoto (1979) | April-79 | | 1 | 5 | 2 | 2 | |
| April 3-4, 1974 | Fujita (1975) | April-74 | 21 | 32 | 30 | 35 | 24 | 6 |
| Pre-1981 Total No. Tors. = 158 | | | 21 | 33 | 35 | 37 | 26 | 6 |
| Post-1981 NGR Data | | | | | | | | |
| Chandler-Lake Wilson MN | NWS Sioux Falls (1992) | Jun-92 | | | | | | 1 |
| Kellerville & Alanreed | Wakimoto (2003) | Jun-95 | | | | 1 | | 1 |
| Moore, OK | NWS Norman (1998) | Oct-98 | | | 1 | | | |
| Central OK, A9 | Spehger (2002) | May-99 | | | | | | 1 |
| June 24, 2003 | NWS Sioux Falls (2003) | Jun-03 | | | 1 | 2 | 1 | |
| Coleridge | Smith (2003) | Jun-03 | | | | | 1 | |
| Walnut, IA | Smith (2004) | May-04 | | 1 | | | | |
| Hallam, NE | NWS Omaha/Valley (2004) | May-04 | | | | | | 1 |
| Clay Co., IA | NWS Sioux Falls (2004) | Jun-04 | | | 1 | 1 | | |
| Beadle Co., SD | NWS Sioux Falls (2006) | Aug-06 | | | 1 | 1 | | |
| Parkersburg, IA | Marshall (2008b) | May-08 | | | | | | 1 |
| Little Sioux Scout Camp | NWS Omaha/Valley (2008) | Jun-08 | | | | | 1 | |
| Pre-1981 Total No. Tors. = 18 | | | 0 | 1 | 4 | 6 | 3 | 4 |
| Total No. NGR Tors. = 176 | | | 21 | 34 | 39 | 43 | 29 | 10 |

We begin by examining how the mean rating of a tornado, conditional on the tornado F/EF scale, varies with path length. The mean rating is computed by averaging the individual ratings along the path length. Figure 3(a) plots tornado path length versus mean rating by F/EF scale for the combined NGR data. The first noticeable trend is that the mean rating decreases with path length. However, the R^2 values are relatively small for F/EF2-F/EF5 tornadoes, indicating that most of the variation in mean PLIV rating is not explained by total path length. For F/EF1 tornadoes, the data spread is tighter and influenced by shorter path length tornadoes with a constant rating. By removing the constant rated F/EF1 and F/EF2 tornadoes², we see lower R^2 values and nearly horizontal fits for these intensities in Figure 3b. The significance of the downward slopes in Figure 3 cannot be deciphered simply from NGR data. The vagaries of rating tornadoes with potential ± 1 (or more) F/EF scale accuracies, the spacing of the ratings, and randomness in tornado intensity variations are all confounded in Figure 3. For now, we leave this as an open question and note simply that it is not

² Removing the constant rated short tornadoes follows from the fact that the average spacing of the PLIV ratings was greater than path lengths of the short tornadoes.

unreasonable to normalize the data by path length, given the inherent limitations of the data.

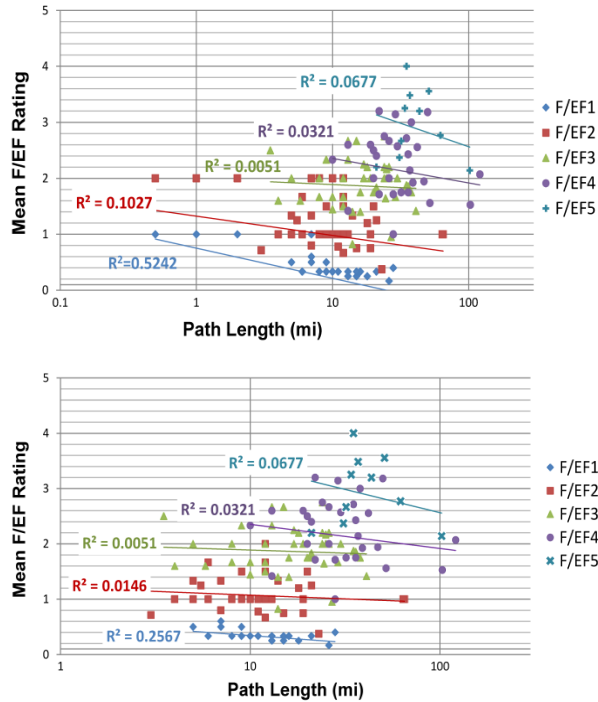


Figure 3. Mean F/EF Rating vs. Path Length for (a) All Tornadoes and (b) Not Including Tornadoes with Constant Intensity

The next step is to compute the F/EF scale fractional path lengths, conditional on the tornado F/EF scale. We sum the lengths of each tornado's local intensity levels and then normalize each tornado by its path length (leaving us with fractions of each local intensity level, for each tornado). We then average the fractions for each local intensity level for tornadoes within each tornado rating. The result is conditional probabilities of the local path length intensity, given the intensity rating of the tornado ($P(I_i^*|F/EF)$). From Figure 3, we know this will be somewhat conservative since the longer tornadoes have lower mean ratings over their path lengths.³ Normalizing by length causes each tornado to have an equal input to the mean fraction summary, regardless of its length. Table 3 summarizes the results of the updated NGR analysis.

Table 3(a) gives the mean fractions for the April 3-4, 1974 (Fujita, 1975) and the Red River Valley data (Fujita and Wakimoto, 1979), Table 3(b) gives the mean fractions for the post 1981 NGR data, and Table 3(c) gives the mean fractions for the combination of the data in Table 3(a) and Table 3(b). The sum of each column is

³ Hence, this approach is conservative relative to the method used by Twisdale (1978) and Twisdale et al. (1978, 1981), which added path length segments within each F Scale.

one, that is $\sum_{i=0}^{F/EF} P(I_i^*|F/EF) = 1$. We see that normalizing the fractions by each tornado produces slightly higher principal diagonals in Table 3(a) vs. Table 1. The principal diagonal values, highlighted in light red in Table 3, are the portions of the path that are rated the same as the tornado. Comparison of the values in Table 3(a) to those in Table 3(b)-(c), shows that the addition of the more recent data minimally affects F/EF1 to F/EF4 tornadoes. This result is largely due to the small numbers of post 1981 F/EF1 to F/EF4 path length damage surveys. The newer data provides more F/EF5 tornadoes to the dataset, and causes the portion of higher local ratings within F/EF5 tornadoes to increase. We note that there are only 2 EF rated tornadoes in the post 1981 NGR data. Hence the NGR PLIV data remains essentially an F scale data set.

Table 3. Mean Fraction Tables: $P(I^*|F/EF)$

| (a) April 3-4, 1974 and Red River Valley NGR Data | | | | | | |
|--|----------------|-------|-------|-------|-------|-------|
| Local PL Intensity | Tornado Rating | | | | | |
| | ≤F0 | F1 | F2 | F3 | F4 | F5 |
| ≤10* | 1.00 | 0.371 | 0.198 | 0.090 | 0.129 | 0.118 |
| 11* | | 0.629 | 0.291 | 0.246 | 0.147 | 0.122 |
| 12* | | | 0.511 | 0.311 | 0.259 | 0.162 |
| 13* | | | | 0.353 | 0.225 | 0.240 |
| 14* | | | | | 0.240 | 0.189 |
| 15* | | | | | | 0.169 |
| No. Tors=158 | 21 | 33 | 35 | 37 | 26 | 6 |
| (b) Post 1981 NGR Data | | | | | | |
| Local PL Intensity | Tornado Rating | | | | | |
| | ≤F0 | F1 | F2 | F3 | F4 | F5 |
| ≤10* | 1.00 | 0.667 | 0.207 | 0.106 | 0.190 | 0.019 |
| 11* | | 0.333 | 0.478 | 0.345 | 0.330 | 0.065 |
| 12* | | | 0.315 | 0.325 | 0.189 | 0.314 |
| 13* | | | | 0.224 | 0.103 | 0.111 |
| 14* | | | | | 0.188 | 0.220 |
| 15* | | | | | | 0.271 |
| No. Tors=18 | 0 | 1 | 4 | 6 | 3 | 4 |
| (c) Combined Non-Geo-Referenced PLIV Data | | | | | | |
| Local PL Intensity | Tornado Rating | | | | | |
| | ≤F0 | F1 | F2 | F3 | F4 | F5 |
| ≤10* | 1.00 | 0.380 | 0.199 | 0.093 | 0.135 | 0.079 |
| 11* | | 0.620 | 0.310 | 0.259 | 0.165 | 0.099 |
| 12* | | | 0.491 | 0.313 | 0.252 | 0.223 |
| 13* | | | | 0.335 | 0.213 | 0.188 |
| 14* | | | | | 0.235 | 0.201 |
| 15* | | | | | | 0.210 |
| No. Tors=176 | 21 | 34 | 39 | 43 | 29 | 10 |

The cumulative mean fraction plot of the combined data is shown in Figure 4. The mean fraction of $P(I_{i < max}^*|F/EF)$ increases with increasing F/EF scale, indicating a smaller fraction of the tornado length has the rated maximum intensity.

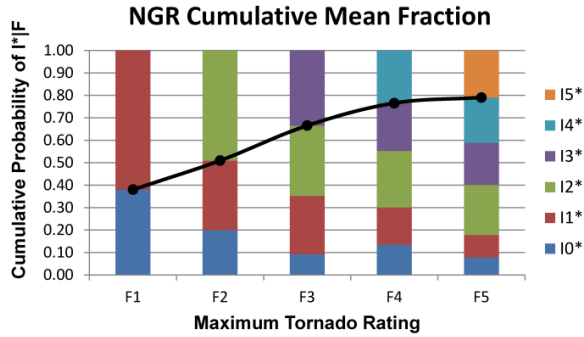


Figure 4. Cumulative Mean Fraction Plot Summarizing the Combined Non-Geo-Referenced Data

The average spacing of the intensity ratings in this data set varied from about 1.4 miles for the Red River Valley tornadoes, 2.4 miles for the post 1981 NGR data, and approximately 4 miles for the April 3-4, 1974 outbreak, producing an average spacing of 3.7 miles. Plots of tornado path length versus the number of ratings along the path are given in Figure 5. We see the consistency of the spacing for the April 1974 and Red River Valley mappings and a bifurcation of the data for the Post 1981 NGR maps. The bifurcation of the Post 1981 data is illustrated by the four F/EF5 tornadoes, where for two tornadoes the average spacing was about 1.25 miles, whereas the other two had average spacing of about 8.8 miles. The F/EF5 main diagonal fractions were notably different, 0.092 vs 0.45, respectively. These differences indicate large uncertainties in the estimation of PLIV mean fractions. The average of these fractions is the $P(15^*|F/EF5)$ value (0.271) in Table 3(b).

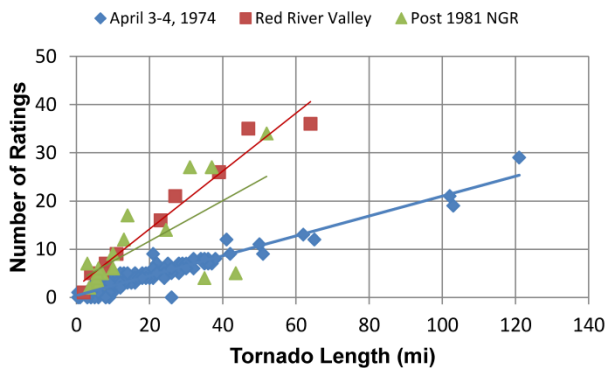


Figure 5. NGR Tornado Path Length vs. the Number of Ratings along Tornado Path and the Linear Regressions

Differences between mappings in parameters such as mean spacing and mean fractions touch on the limitations of damage-based PLIV and the inherent inconsistencies that result from damage-based mapping. The analysis of the NGR PLIV data showed that tornado maps with larger spacing between ratings

tend to result in larger portions of higher ratings in their mean fraction summaries. More data is needed, coupled with analysis of F/EF scale rating uncertainties, to improve the NGR modeling of PLIV.

3. BACKGROUND ON THE NWS DAT

The NWS Damage Assessment Toolkit (DAT) (NOAA, 2016) is a GIS based framework that is used to collect and store geo-referenced tornado data. Tornado data is entered into the DAT during NWS damage surveys, where the surveyors have a hand held device that allows them to enter geo-tagged details for each damage indicator (DI), including specifics on the DI, the rating, the degree of damage (DOD), and photos of the DI. In some cases, contours of the varying damage levels and/or the estimated tornado path line are also drawn.

The DAT has been beneficial in increasing the efficiency and accuracy of tornado damage surveys, as well as providing a central database for detailed tornado damage survey data. Data exists in the publicly available DAT database from 2008 to present, although the amount of data has largely increased in the more recent years as the DAT has progressed in its development and as more Weather Forecast Offices (WFOs) have adopted the toolkit. Figure 6 shows the location of the DAT tornadoes contained in the processed dataset (processing described below) that we use as a starting point in this analysis. It is clear that some WFOs use the DAT and some still have yet to adopt it. We therefore must keep in mind that the DAT data is not fully representative of the entire United States, but clearly covers regions with the highest tornado risk.



Figure 6. DAT Tornadoes

The NWS states that the DAT database is a preliminary database. Each path line, DI, and contour exists within the DAT as a separate geometry entity. The DAT data was downloaded in March of 2015 from 2008 through February, 2015. Examination of the DAT data found that many of the DIs, paths, and contours were not labeled with a unique event ID number. The event ID number allows a user to link together all of the geometries that

exist for a single tornado without displaying the data in a geographic interface, allowing the DIs to be processed by tornado event.

In order to be able to systematically use the data, the DIs and tornado paths/contours were geographically plotted in ArcGIS, and based on location and date, the DIs, paths, and contours belonging to a single event were manually given a unique event ID number. The manual matching was done to the best of our ability, although especially for cases of tornado outbreaks, it was at times difficult to distinguish which DIs belonged to the same event. Hence, our matching may not be perfect.

The level of data entered into the DAT also varies from tornado to tornado. Some of the tornado data consists of highly detailed tornado surveys, while other tornado data may only consist of the starting and ending locations, or a few sparse damage indicators along the path.

4. GEO-REFERENCED PLIV DATA

Although the geo-referenced DAT data was not necessarily created to form a systematic PLIV data source, the data nevertheless provides an opportunity for exploring PLIV. The geo-referenced PLIV analysis was based on the processed NWS DAT data for the years 2008-2015. Comparison of the DAT events with the SPC database resulted in 734 events validated by location and date, from 2010 to 2014. The number of verified tornadoes for each EF-Scale is given in Table 4.

The path lengths of the verified DAT events were compared to the tornado path lengths in the SPC database by EF-Scale, as given in Table 4. The DAT mean path lengths in Table 4 are slightly longer (for all but EF5, for which there is only one tornado in the DAT data). Based on statistical tests (F-tests for equivalence of variances and unpaired t-tests for equivalence of means), the DAT data is representative of the SPC data, except for F/EF0. Hence, from a path length perspective, we assume the DAT data is representative for a PLIV analysis.

Table 4. Number of Events and Mean and Standard Deviation of Path Length for Verified DAT Events and SPC Events (2010-2014). The mean (weighted by SPC EF-Scale fractions) is given for All DAT Events.

| Tor. Rating | Verified DAT Events | | | SPC Events (2010-2014) | | |
|-------------|---------------------|------------------|-------|------------------------|------------------|-------|
| | No. Events | Path Length (mi) | | No. Events | Path Length (mi) | |
| | | Mean | SD | | Mean | SD |
| EF0 | 184 | 2.13 | 2.64 | 3118 | 1.39 | 2.31 |
| EF1 | 360 | 4.98 | 5.80 | 1812 | 4.40 | 4.97 |
| EF2 | 123 | 8.64 | 7.88 | 563 | 8.70 | 9.09 |
| EF3 | 49 | 22.00 | 16.68 | 156 | 18.72 | 15.82 |
| EF4 | 17 | 38.69 | 32.19 | 49 | 32.84 | 31.69 |
| EF5 | 1 | 37.07 | 0.00 | 7 | 47.51 | 37.38 |
| All | 734 | 4.58 | 10.93 | 5705 | 3.87 | 7.58 |

DI PLIV ANALYSIS

An automated process was used to create PLIV catalogs for the 734 geo-referenced tornadoes. Before the PLIV data was extracted to form catalogs, Albers equal-area conic projection was used to transform the latitude/longitude coordinate system to an x-y coordinate system. In order to sequence the DIs in the positive tornado path direction, a least squares line was fit to the DI points in each tornado, and each tornado was rotated about this line, as shown in Figure 7(a)-(b). Following this coordinate transformation and rotation, the tornado paths were discretized into sections of a specific kernel discretization length (dx) and the maximum DI EF-rating was determined for each kernel length; kernel lengths with no DIs were labeled as unknown. The following six different cases of kernel size were investigated in the analysis: dx = 0.25mi., 0.5mi., 1mi., 2mi., 3mi., and 4mi. This discretization and rating determination process is illustrated in Figure 8.

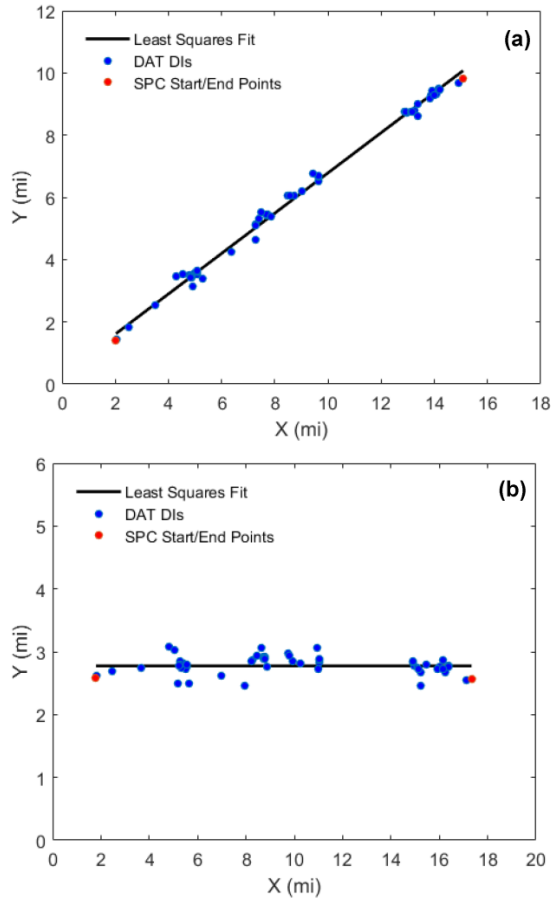


Figure 7. Illustration of Coordinate Rotation about Tornado Paths (a) Latitude/Longitude Space Transformed to X-Y Space, (b) X-Y Coordinates Rotated so Path Direction is Aligned with X-Axis

Regarding unknown kernel lengths, our approach is to estimate the ratings by linearly interpolating between kernels of unknown rating, assuming persistence of intensity. This process of estimating the unknowns is illustrated in Figure 9. Step 2 in Figure 9 shows that we

begin by combining consecutive segments with the same rating into one rating of a larger segment length. Next, we assume persistence in Step 3 and linearly interpolate to estimate the ratings of unknown segments, and once again combine consecutive segments with the same rating in Step 4.

Mean fraction table summaries of the catalogs created with each dx value are given in Table 5. We see that the results vary significantly with kernel length. For small dx , the principal diagonal fractions drop off rapidly with increasing EF scale. However, we also note that for $dx = 0.25$ mile, the mode of the local intensity is mostly either EF0 or EF1, i.e., I0* or I1*, according to our notation. Further, for $dx = 0.5$ and 1 mile, the local intensity of I1* and I2* are the modes for EF1-EF3 and EF4 tornadoes, respectively. These results suggest that strong and intense tornadoes are mostly weak during their life cycle. Another contributing factor is that the spacing of ratings along the path length is highly variable and subject to the available time and accessibility by the surveyor.

Table 5 exhibits the expected monotonic increase in the diagonal values for larger dx , which results from our persistence assumption. For the longer dx values, the modes for EF1-EF4 equal the tornado rating. At $dx = 4$ miles, the principal diagonal results are close to the NGR results (Table 3), which, as noted previously, correspond to an average rating spacing of about 3.7 miles. This general agreement of the NGR and GR principal diagonal data for similar spacing of maximum local intensity is significant since the processed GR data includes the effect of over 10,000 individual EF ratings along 734 tornadoes by different meteorologists.



Figure 8. Illustration of Path Discretization and Maximum DI Determination

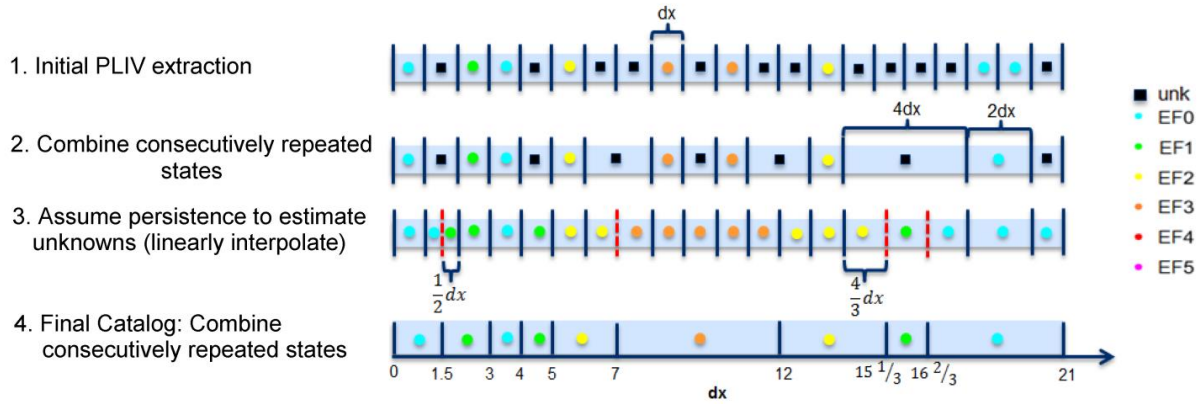


Figure 9. Illustration of Unknown Rating Estimation Process

Table 5. EF Scale DAT $P(I^*|EF)$ for Different Kernel (dx) Lengths

| (a) $dx = 0.25$ mi | | (b) $dx = 0.5$ mi | | | | | | | | | | | |
|--------------------|----------------|-------------------|------|------|------|------|--------------------|----------------|------|------|------|------|------|
| Local PL Intensity | Tornado Rating | | | | | | Local PL Intensity | Tornado Rating | | | | | |
| | EF0 | EF1 | EF2 | EF3 | EF4 | EF5 | | EF0 | EF1 | EF2 | EF3 | EF4 | EF5 |
| I0* | 1.00 | 0.30 | 0.16 | 0.19 | 0.17 | 0.64 | I0* | 1.00 | 0.25 | 0.16 | 0.16 | 0.14 | 0.59 |
| I1* | | 0.70 | 0.57 | 0.42 | 0.25 | 0.07 | I1* | | 0.75 | 0.53 | 0.41 | 0.24 | 0.07 |
| I2* | | | 0.27 | 0.30 | 0.30 | 0.05 | I2* | | | 0.31 | 0.30 | 0.31 | 0.06 |
| I3* | | | | 0.09 | 0.22 | 0.07 | I3* | | | | 0.13 | 0.22 | 0.05 |
| I4* | | | | | 0.07 | 0.13 | I4* | | | | | 0.09 | 0.15 |
| I5* | | | | | | 0.03 | I5* | | | | | | 0.07 |

| (c) $dx = 1$ mi | | (d) $dx = 2$ mi | | | | | | | | | | | |
|--------------------|----------------|-----------------|------|------|------|------|--------------------|----------------|------|------|------|------|------|
| Local PL Intensity | Tornado Rating | | | | | | Local PL Intensity | Tornado Rating | | | | | |
| | EF0 | EF1 | EF2 | EF3 | EF4 | EF5 | | EF0 | EF1 | EF2 | EF3 | EF4 | EF5 |
| I0* | 1.00 | 0.19 | 0.12 | 0.13 | 0.12 | 0.59 | I0* | 1.00 | 0.09 | 0.08 | 0.10 | 0.07 | 0.00 |
| I1* | | 0.81 | 0.47 | 0.39 | 0.20 | 0.05 | I1* | | 0.91 | 0.37 | 0.36 | 0.14 | 0.63 |
| I2* | | | 0.41 | 0.30 | 0.32 | 0.05 | I2* | | | 0.56 | 0.28 | 0.32 | 0.00 |
| I3* | | | | 0.18 | 0.20 | 0.03 | I3* | | | | 0.26 | 0.23 | 0.05 |
| I4* | | | | | 0.16 | 0.14 | I4* | | | | | 0.24 | 0.16 |
| I5* | | | | | | 0.14 | I5* | | | | | | 0.16 |

| (e) $dx = 3$ mi | | (f) $dx = 4$ mi | | | | | | | | | | | |
|--------------------|----------------|-----------------|------|------|------|------|--------------------|----------------|------|------|------|------|------|
| Local PL Intensity | Tornado Rating | | | | | | Local PL Intensity | Tornado Rating | | | | | |
| | EF0 | EF1 | EF2 | EF3 | EF4 | EF5 | | EF0 | EF1 | EF2 | EF3 | EF4 | EF5 |
| I0* | 1.00 | 0.06 | 0.06 | 0.05 | 0.06 | 0.00 | I0* | 1.00 | 0.04 | 0.04 | 0.07 | 0.05 | 0.56 |
| I1* | | 0.94 | 0.29 | 0.30 | 0.13 | 0.58 | I1* | | 0.96 | 0.20 | 0.23 | 0.10 | 0.00 |
| I2* | | | 0.66 | 0.31 | 0.30 | 0.00 | I2* | | | 0.76 | 0.26 | 0.24 | 0.00 |
| I3* | | | | 0.35 | 0.23 | 0.00 | I3* | | | | 0.44 | 0.27 | 0.00 |
| I4* | | | | | 0.28 | 0.17 | I4* | | | | | 0.34 | 0.22 |
| I5* | | | | | | 0.25 | I5* | | | | | | 0.22 |

CONTOUR PLIV ANALYSIS

PLIV was also investigated for contour data in the DAT by using ArcGIS to measure the lengths of each local rating for tornadoes with contour data. The contour data consists of 110 of the 734 verified DAT tornadoes that have more than one associated intensity contour in addition to their DI data.

Figure 10 illustrates how the lengths of the maximum rated contour along the path length of the tornado were measured. Catalogs were created by recording the ratings and their respective lengths in the order that they occurred. The mean fraction summaries of the contour PLIV analysis are given in Table 6. **Error! Reference source not found.**

than those in Table 5. For EF1 and EF2 tornadoes, the relative fraction of I0* and I1* is significantly lower in Table 5 for all dx values investigated. We conclude that the contouring process is not representative of the DAT tornado PLIV analysis. It appears that EF0 contours may have been extended to areas of unknown damage that were not investigated. Hence, for PLIV modeling purposes, we will not further consider the DAT contour data.

Table 6. Mean Fraction Table: $P(I^*|EF)$ Summarizing Contour PLIV Analysis

| Local PL Intensity | Tornado Rating | | | | | |
|--------------------|----------------|------|------|------|------|------|
| | EF0 | EF1 | EF2 | EF3 | EF4 | EF5 |
| I0* | 1.00 | 0.65 | 0.53 | 0.29 | 0.32 | 0.47 |
| I1* | | 0.35 | 0.32 | 0.45 | 0.28 | 0.08 |
| I2* | | | 0.16 | 0.15 | 0.28 | 0.02 |
| I3* | | | | 0.12 | 0.09 | 0.18 |
| I4* | | | | | 0.03 | 0.24 |
| I5* | | | | | | 0.01 |

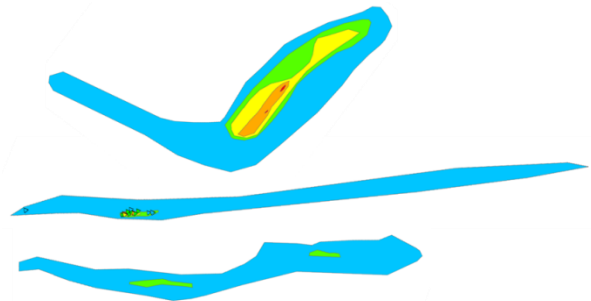


Figure 11. Example Tornado Contours with Large EF0 Portions

The highlighted diagonal in Table 6 shows that the contour PLIV analysis produces very low persistence of maximum tornado intensity. We also see very high persistence of EF0 for all EF rated tornadoes. The persistence of EF0 suggests that there were no DIs for significant lengths of these DAT events, that these areas were not investigated, and/or that unrated/unknown DIs were mapped as EF0. Figure 11 shows several example tornadoes with large portions of EF0 contours. In particular, the I0* contour fractions in **Error! Reference source not found.** are much higher

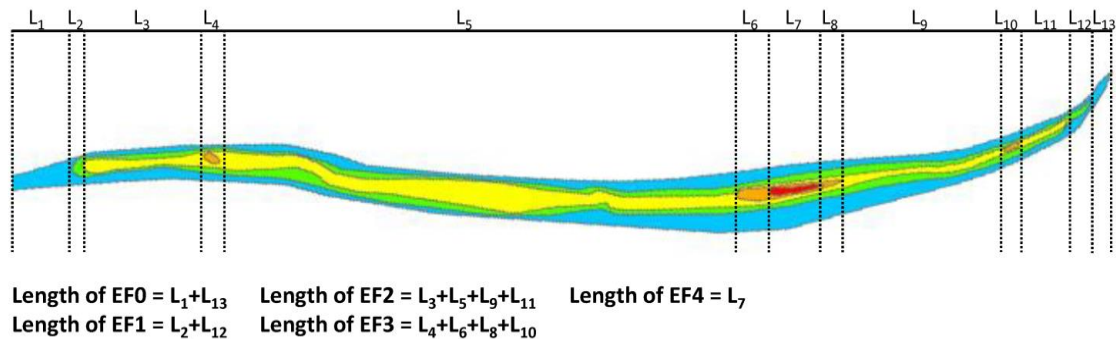


Figure 10. Example Illustration of how PLIV Catalogs are created from Contour Data

5. A PLIV MODEL BASED ON INTENSITY PERSISTENCE

A cumulative mean fraction plot, comparing the NGR and DI GR results, is given in Figure 12. This figure shows all the data in Table 3(c) and Table 5 as stacked, cumulative mean fraction distributions. For the geo-referenced DI method, longer discretization segments naturally produce results with higher values for the principal diagonal, $P(I^*|F/EF = I^*)$. The downward progression with increasing dx from left to right in Figure 12 follows our persistence assumption. At dx = 4 miles, we see that the DAT data compares reasonably well to the NGR data for F/EF3-F/EF5. For example, the principal diagonal values for dx=4 miles vs. the NGR data are 0.44 vs. 0.34 for EF3, 0.34 vs. 0.24 for EF4, and 0.22 vs. 0.21 for EF5. However, the DAT data has significantly higher maximum intensity fractions for EF1 and EF2, with principal diagonal fractions of 0.96 vs. 0.62 and 0.76 vs. 0.49, respectively. These high fractions do not seem reasonable and likely stem from some of the aforementioned discussions regarding EF0 ratings in the DAT.

It is important to note that the DAT PLIV analysis of 734 tornadoes, when processed with a kernel length of 4 miles, compares well to the updated NGR data (176 tornadoes), which has a mean spacing length of 3.7 miles. The NGR method has consistent fractions of local path intensity across F/EF-scales, with results that show reasonable persistence of larger intensities.

Figure 13(a) shows a 3-D mean fraction probability plots of the DAT analysis for the 4 mile kernel length. We see a number of anomalies, including a bipolar I0* distribution with peaks at F0 and F5 and very small fractions in between. Also, the F5 distribution has an usual gap for I1*, I2* and I3*. Figure 13(b) shows the updated NGR results from Table 3(c). Although the mean principal diagonal fraction conditional probabilities are very similar, the smoothness and consistency of the updated NGR data is apparent. The NGR dataset is largely based on maximum intensity ratings for consistent length sections of the tornado path. The DAT data was not developed from that perspective and hence, would not be expected to provide results that are as consistently smooth as the NGR data.

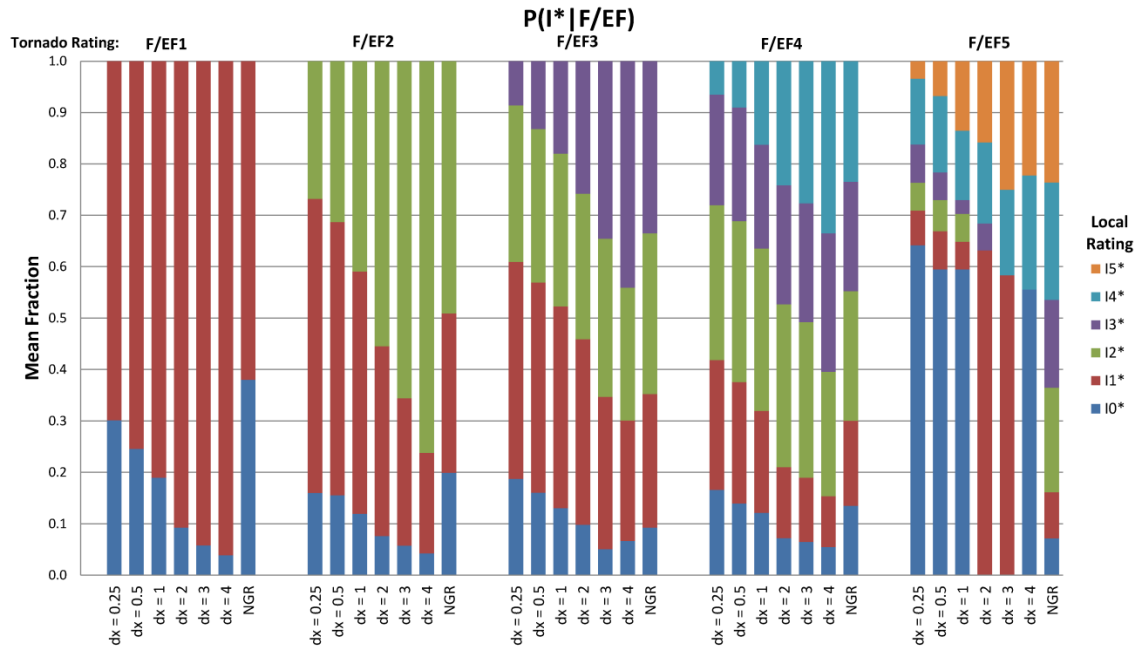


Figure 12. Cumulative Mean Fraction Plot Summarizing NGR, DI GR, and Contour GR Results

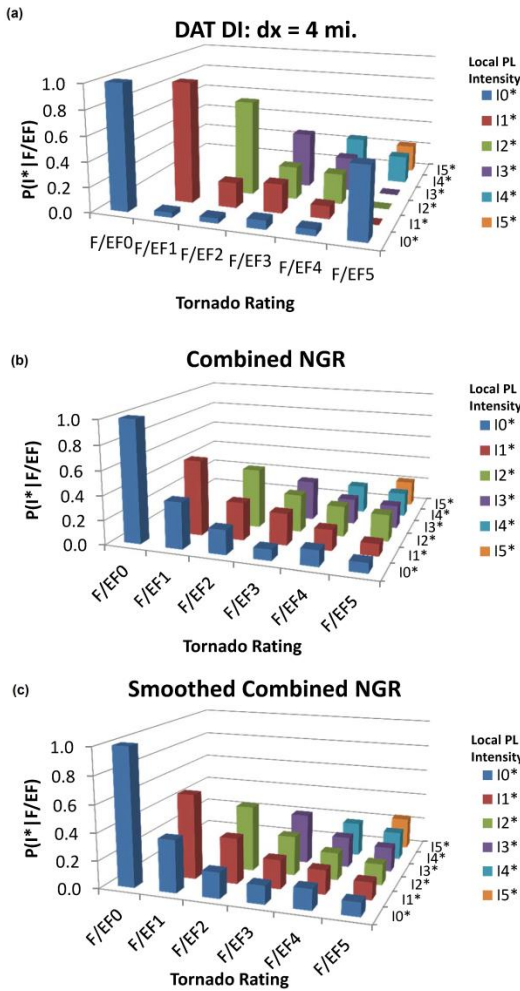


Figure 13. Mean Fraction Probabilities by Tornado Rating for (a) DI DAT Analysis with dx = 4 mi., (b) Combined NGR Data, (c) Smoothed Combined NGR Data

Based on the above discussions, we suggest use of the NGR data for PLIV modeling. We believe that since the majority of the NGR data had aerial surveys for purposes of mapping intensity variations, it makes that data our best source. Also, as noted previously, the DAT GR data reduces to a very similar set of principal diagonal data for a similar kernel length.

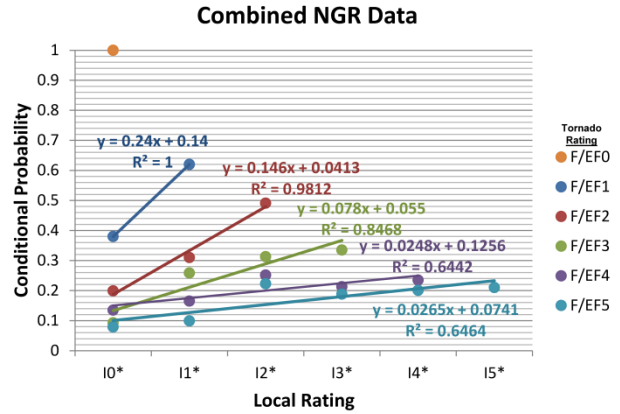


Figure 14. Combined NGR Conditional Probability vs. Local Rating

The NGR conditional probabilities (the mean fraction columns in Table 3(c)) are plotted by F/EF scale in Figure 14. We have smoothed this data by fitting linear models to the $P(I_i^*|F/EF)$ distributions. This smoothing removes the small non-linearities in the data and results in very minor changes to the probabilities. The final mean fraction summary of the smoothed NGR data is illustrated in Figure 13(c). Tabular results of the final smoothed PLIV conditional probabilities are given in Table 7. Table 7(a) shows the smoothed mean fractions, Table 7(b) shows the standard deviations, and Table 7(c) shows the coefficient of variation of each entry. The COV statistics suggest very large uncertainties in the mean fractions. These uncertainties in the mean fractions can be statistically modeled using the data in Table 7. The minimums of the principal diagonal mean values in Table 7(a) are 0.167, 0.063, 0.059, 0.053, and 0.074 for EF1 through EF5, as shown in Table 7(d). The maximums of the principal diagonal mean values in Table 7(a) are 1, 1, 0.75, 0.55, and 0.5 for EF1 through EF5, as shown in Table 7(e).

Table 7. (a) Mean, (b) Standard Deviation, (c) Coefficient of Variation, (d) Minimum, and (e) Maximum of $P(I^*|F)$ for Smoothed, Combined NGR Data

| (a) Mean | | | | | | |
|-------------------------------------|----------------|-------|-------|-------|-------|-------|
| Local PL Intensity | Tornado Rating | | | | | |
| | F/EF0 | F/EF1 | F/EF2 | F/EF3 | F/EF4 | F/EF5 |
| 10* | 1.00 | 0.380 | 0.187 | 0.133 | 0.150 | 0.100 |
| 11* | | 0.620 | 0.333 | 0.211 | 0.175 | 0.127 |
| 12* | | | 0.480 | 0.289 | 0.200 | 0.153 |
| 13* | | | | 0.367 | 0.225 | 0.180 |
| 14* | | | | | 0.250 | 0.207 |
| 15* | | | | | | 0.233 |
| No. Tors=176 | 21 | 34 | 39 | 43 | 29 | 10 |
| (b) Standard Deviation | | | | | | |
| Local PL Intensity | Tornado Rating | | | | | |
| | F/EF0 | F/EF1 | F/EF2 | F/EF3 | F/EF4 | F/EF5 |
| 10* | 0.000 | 0.332 | 0.205 | 0.198 | 0.155 | 0.113 |
| 11* | | 0.332 | 0.266 | 0.158 | 0.134 | 0.114 |
| 12* | | | 0.304 | 0.168 | 0.117 | 0.121 |
| 13* | | | | 0.174 | 0.171 | 0.112 |
| 14* | | | | | 0.126 | 0.184 |
| 15* | | | | | | 0.158 |
| (c) Coefficient of Variation | | | | | | |
| Local PL Intensity | Tornado Rating | | | | | |
| | F/EF0 | F/EF1 | F/EF2 | F/EF3 | F/EF4 | F/EF5 |
| 10* | 0.000 | 0.873 | 1.096 | 1.488 | 1.031 | 1.129 |
| 11* | | 0.535 | 0.798 | 0.751 | 0.767 | 0.898 |
| 12* | | | 0.633 | 0.582 | 0.583 | 0.793 |
| 13* | | | | 0.474 | 0.759 | 0.623 |
| 14* | | | | | 0.505 | 0.889 |
| 15* | | | | | | 0.679 |
| (d) Minimum | | | | | | |
| Local PL Intensity | Tornado Rating | | | | | |
| | F/EF0 | F/EF1 | F/EF2 | F/EF3 | F/EF4 | F/EF5 |
| 10* | 1.000 | 0.000 | 0.000 | 0.000 | 0.000 | 0.000 |
| 11* | | 0.167 | 0.000 | 0.000 | 0.000 | 0.000 |
| 12* | | | 0.063 | 0.000 | 0.000 | 0.000 |
| 13* | | | | 0.059 | 0.000 | 0.000 |
| 14* | | | | | 0.053 | 0.000 |
| 15* | | | | | | 0.074 |
| (e) Maximum | | | | | | |
| Local PL Intensity | Tornado Rating | | | | | |
| | F/EF0 | F/EF1 | F/EF2 | F/EF3 | F/EF4 | F/EF5 |
| 10* | 1.000 | 0.833 | 0.688 | 0.500 | 0.600 | 0.200 |
| 11* | | 1.000 | 0.800 | 0.667 | 0.500 | 0.250 |
| 12* | | | 1.000 | 0.800 | 0.538 | 0.600 |
| 13* | | | | 0.750 | 0.800 | 0.333 |
| 14* | | | | | 0.545 | 0.519 |
| 15* | | | | | | 0.500 |

6. PLIV CATALOGS AND SIMULATED WIND SPEEDS

The previous analyses have focused on developing PLIV conditional probabilities, which represent mean fractions of normalized tornado length, $P(I_i^*|F/EF)$. In this section, we provide the data used to develop the

mean fractions in the form of PLIV “catalogues.” A PLIV “catalog” refers to the sequential record of F/EF scale ratings for an individual tornado and the associated position on the path length that corresponds to the intensity. When normalized by path length, the cumulative path position is a fraction bounded by zero to one. For example, a catalogue of intensities (say, 0, 1, 1, 2, and 0) has an associated string of normalized starting positions (say, 0.0, 0.2, 0.4, 0.6, and 0.8).

PLIV catalogues are useful for modeling large spatially-distributed systems, where the tornado intensity variation along the path may be important in the risk analysis. For example, critical facilities (such as emergency operation centers, hospitals, public shelters, etc.) may be separated by miles or tens of miles within a municipality. Electrical substations and transmission line systems also cover large areas.

Table 8 shows the PLIV sequence for each tornado in the updated F1-F5 NGR dataset (155 Tornadoes = 176 total tornadoes - 21 F0 tornadoes). These data illustrate the actual catalogues by normalized path length. The PLIV catalogs are grouped by F/EF scale, based on the maximum rating within the tornado. The intensity state transition sequences illustrated in Table 8 have a large random component. We generally see fewer intensity transitions for the lower F/EF scales, which also have shorter lengths on average. One can also readily see the longer tornadoes that were mapped with many intensity segments.

A visual analysis of Table 8 suggests that the maximum intensity of the NGR tornadoes typically occurs near the center of the path. This observation is consistent with the generally recognized tornado life cycle characteristics of a formation stage, mature stage, and dissipation stage. We performed a simple analysis by dividing the catalogs into thirds. We found that the maximum intensity damage rating was observed 45, 90, and 52% of the time within each sequential one third of the normalized path length, with similar trends observed when broken out by F/EF-Scale. The middle third is about twice as likely to have a maximum rated segment as the starting and ending thirds. In addition, we counted the number of events that had a unimodal maximum rating type of damage-based life cycle and 85% had this characteristic. These results (formative, mature, dissipative stage) tend to support general observations of tornado life cycles noted in the literature (e.g., Golden and Purcell (1978), Grazulis (2001), Wakimoto et al. (2003), Atkins et al. (2014), etc.).

We also counted the number of events that experienced more than one peak in intensity, not necessarily equal to the maximum intensity, and 29% exhibited this behavior.

Hence, the NGR catalogues include macro-level strong-weak-strong life cycles, which have been observed from radar and photogrammetric analysis (e.g. Burgess et al. (2002), Kosiba et al. (2013), and Wakimoto et al. (2011)).

These NGR PLIV catalogs can be implemented for use in tornado damage swath modeling. The catalogs can be used to model tornado PLIV by randomly selecting a PLIV catalog, conditional on F/EF scale. The catalogues can also be implemented with a length dependence correlation within the F/EF scale dependence. With either approach, the tornado intensity will vary along the tornado path length based on the sampled PLIV catalog in Table 8.

An example of the use of the PLIV catalogue modeling approach is illustrated in Figure 15. A sampled

catalogue is illustrated in Figure 15 (a), in which the life cycle macro-level intensity transitions are 3-5-4-2-2-0. In tornado wind speed risk modeling, we convert the F/EF ratings in the catalogs to wind speeds. A wind speed for each F/EF segment is sampled from a wind speed given damage probability distribution model for that damage intensity. An advantage of this approach is that the wind speed distribution given damage intensity is separate from the PLIV model. The sampled wind speeds are assigned to the midpoints of the segments and a spline fitting method is used to smooth the wind speeds between segment midpoints. This process is illustrated in Figure 15 using the EF scale wind speed ranges. Future papers will describe this tornado swath modeling process in more detail.

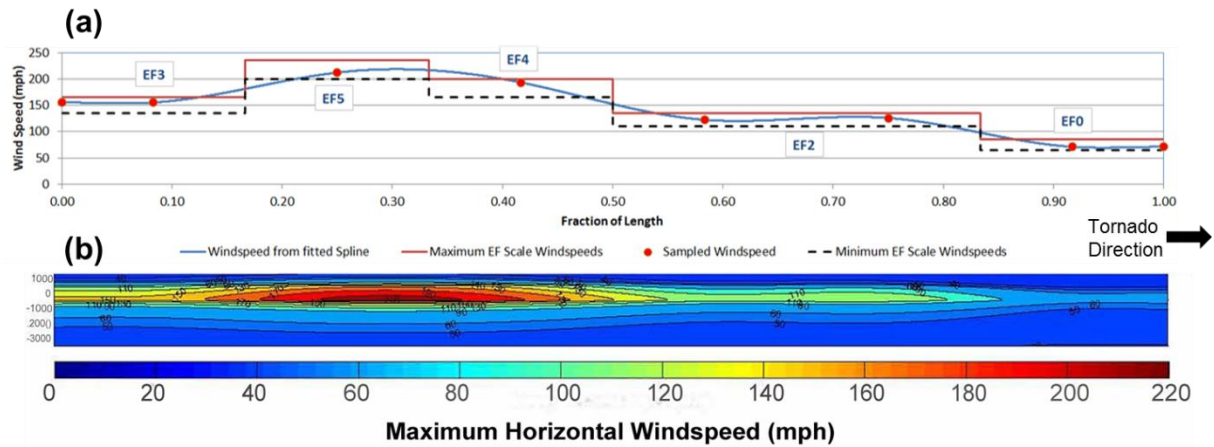


Figure 15. (a) A Sample Spline Fitted Catalog, and its (b) Simulated Tornado Wind speed Swath

Table 8. Listings of the 155 F/EF1-F/EF5 NGR Catalogs. Catalogs are grouped by tornado rating, each line is a catalog for a tornado, and the ratings are shown in the order they occur. The normalized length of each rating is also shown within each catalog, where the left side of the table represents the start of the tornado and the right side of the table represents the tornado end point.

| F/EF | N | PL (mi.) | Normalized Path Length | | | | | | | |
|----------------|----|----------|------------------------|-----|---|-----|---|-----|---|---|
| | | | 0 | 0.5 | 1 | 1.5 | 2 | 2.5 | 3 | 1 |
| F/EF1 Catalogs | 1 | 15 | 0 | 1 | 0 | 0 | | | | |
| | 2 | 13 | 1 | 0 | 0 | | | | | |
| | 3 | 8 | 0 | 1 | 0 | | | | | |
| | 4 | 8 | 0 | 1 | 0 | | | | | |
| | 5 | 16 | 0 | 0 | 1 | | | | | |
| | 6 | 7 | 0 | 1 | | | | | | |
| | 7 | 13 | 0 | 1 | 0 | | | | | |
| | 8 | 0.5 | 1 | | | | | | | |
| | 9 | 13 | 0 | 0 | 1 | 0 | | | | |
| | 10 | 21 | 0 | 1 | 1 | 0 | 1 | 0 | 0 | 0 |
| | 11 | 9 | 0 | 1 | 0 | | | | | |
| | 12 | 7 | 1 | | | | | | | |
| | 13 | 10 | 1 | | | | | | | |
| | 14 | 4 | 1 | | | | | | | |
| | 15 | 15 | 0 | 0 | 1 | | | | | |
| | 16 | 26 | 0 | 0 | 1 | 0 | 0 | 0 | | |
| | 17 | 10 | 0 | 1 | 0 | | | | | |
| | 18 | 4 | 1 | | | | | | | |
| | 19 | 28 | 0 | 1 | 0 | 1 | 0 | | | |
| | 20 | 11 | 0 | 1 | 0 | | | | | |
| | 21 | 6 | 1 | | | | | | | |
| | 22 | 1 | 1 | | | | | | | |
| | 23 | 4 | 1 | | | | | | | |
| | 24 | 9 | 0 | 1 | | | | | | |
| | 25 | 1 | 1 | | | | | | | |
| | 26 | 2 | 1 | | | | | | | |
| | 27 | 5 | 1 | 0 | | | | | | |
| | 28 | 9 | 1 | | | | | | | |
| | 29 | 0.5 | 1 | | | | | | | |
| | 30 | 0.5 | 1 | | | | | | | |
| | 31 | 18 | 0 | 0 | 1 | 0 | | | | |
| | 32 | 1 | 1 | | | | | | | |
| | 33 | 7 | 1 | 1 | 1 | 0 | 0 | | | |
| | 34 | 6 | 0 | 0 | 1 | 0 | 1 | 0 | | |
| F/EF2 Catalogs | 35 | 7 | 1 | 2 | 1 | | | | | |
| | 36 | 21 | 2 | 1 | 2 | 0 | | | | |
| | 37 | 2 | 2 | | | | | | | |
| | 38 | 10 | 1 | 2 | 1 | 0 | | | | |
| | 39 | 19 | 0 | 1 | 2 | 1 | | | | |
| | 40 | 11 | 1 | 2 | 0 | | | | | |
| | 41 | 7 | 2 | | | | | | | |
| | 42 | 12 | 0 | 2 | 0 | | | | | |
| | 43 | 8 | 2 | | | | | | | |
| | 44 | 0.5 | 2 | | | | | | | |
| | 45 | 6 | 1 | 2 | 0 | | | | | |
| | 46 | 15 | 0 | 1 | 2 | 0 | | | | |
| | 47 | 5 | 1 | 2 | 1 | | | | | |
| | 48 | 10 | 2 | 2 | | | | | | |

| | | | | | | | | | | | | | | | | | | | | | | | | | | | | | | | | | | | | | | |
|-----|-----|---|---|---|---|---|---|---|---|---|---|---|---|---|---|---|---|---|---|---|---|---|---|---|---|---|---|---|---|---|---|---|---|---|---|---|---|---|
| 49 | 14 | 1 | 2 | 1 | | | | | | | | | | | | | | | | | | | | | | | | | | | | | | | | | | |
| 50 | 18 | 1 | 1 | 1 | 2 | 1 | | | | | | | | | | | | | | | | | | | | | | | | | | | | | | | | |
| 51 | 9 | 1 | 2 | | | | | | | | | | | | | | | | | | | | | | | | | | | | | | | | | | | |
| 52 | 12 | 2 | 2 | | | | | | | | | | | | | | | | | | | | | | | | | | | | | | | | | | | |
| 53 | 20 | 1 | 2 | 2 | 1 | | | | | | | | | | | | | | | | | | | | | | | | | | | | | | | | | |
| 54 | 13 | 1 | 2 | 0 | | | | | | | | | | | | | | | | | | | | | | | | | | | | | | | | | | |
| 55 | 12 | 1 | 2 | | | | | | | | | | | | | | | | | | | | | | | | | | | | | | | | | | | |
| 56 | 12 | 1 | 2 | 0 | | | | | | | | | | | | | | | | | | | | | | | | | | | | | | | | | | |
| 57 | 1 | 2 | | | | | | | | | | | | | | | | | | | | | | | | | | | | | | | | | | | | |
| 58 | 4 | 2 | 0 | | | | | | | | | | | | | | | | | | | | | | | | | | | | | | | | | | | |
| 59 | 2 | 2 | | | | | | | | | | | | | | | | | | | | | | | | | | | | | | | | | | | | |
| 60 | 12 | 1 | 2 | 2 | | | | | | | | | | | | | | | | | | | | | | | | | | | | | | | | | | |
| 61 | 19 | 1 | 0 | 2 | 0 | | | | | | | | | | | | | | | | | | | | | | | | | | | | | | | | | |
| 62 | 65 | 0 | 0 | 0 | 0 | 1 | 2 | 1 | 2 | 1 | 2 | 2 | 1 | | | | | | | | | | | | | | | | | | | | | | | | | |
| 63 | 9 | 1 | 2 | 0 | | | | | | | | | | | | | | | | | | | | | | | | | | | | | | | | | | |
| 64 | 5 | 0 | 2 | | | | | | | | | | | | | | | | | | | | | | | | | | | | | | | | | | | |
| 65 | 23 | 0 | 1 | 0 | 0 | 0 | 1 | 0 | 0 | 0 | 0 | 0 | 2 | 0 | 1 | 1 | 0 | | | | | | | | | | | | | | | | | | | | | |
| 66 | 8 | 0 | 1 | 1 | 2 | 2 | 1 | 1 | 1 | 1 | 1 | 1 | 1 | 1 | 0 | 1 | 1 | 1 | 2 | 2 | 2 | 1 | 0 | | | | | | | | | | | | | | | |
| 67 | 64 | 0 | 0 | 0 | 1 | 1 | 1 | 1 | 2 | 2 | 2 | 1 | 2 | 1 | 1 | 1 | 1 | 0 | 1 | 0 | 1 | 0 | 1 | 2 | 1 | 1 | 1 | 1 | 1 | 0 | 1 | 1 | 1 | 2 | 2 | 2 | 1 | 0 |
| 68 | 2 | 2 | | | | | | | | | | | | | | | | | | | | | | | | | | | | | | | | | | | | |
| 69 | 11 | 0 | 1 | 1 | 1 | 0 | 0 | 1 | 2 | 1 | | | | | | | | | | | | | | | | | | | | | | | | | | | | |
| 70 | 6 | 1 | 2 | 2 | | | | | | | | | | | | | | | | | | | | | | | | | | | | | | | | | | |
| 71 | 7 | 0 | 0 | 1 | 1 | 2 | | | | | | | | | | | | | | | | | | | | | | | | | | | | | | | | |
| 72 | 5.5 | 1 | 2 | 1 | 1 | | | | | | | | | | | | | | | | | | | | | | | | | | | | | | | | | |
| 73 | 3 | 0 | 1 | 0 | 1 | 2 | 1 | 0 | | | | | | | | | | | | | | | | | | | | | | | | | | | | | | |
| 74 | 8 | 1 | 2 | 3 | 2 | | | | | | | | | | | | | | | | | | | | | | | | | | | | | | | | | |
| 75 | 19 | 0 | 2 | 3 | 3 | 2 | | | | | | | | | | | | | | | | | | | | | | | | | | | | | | | | |
| 76 | 8 | 1 | 3 | 1 | | | | | | | | | | | | | | | | | | | | | | | | | | | | | | | | | | |
| 77 | 17 | 1 | 2 | 3 | 2 | | | | | | | | | | | | | | | | | | | | | | | | | | | | | | | | | |
| 78 | 26 | 1 | 2 | 3 | 3 | 2 | 1 | | | | | | | | | | | | | | | | | | | | | | | | | | | | | | | |
| 79 | 36 | 2 | 2 | 1 | 3 | 3 | 2 | 0 | | | | | | | | | | | | | | | | | | | | | | | | | | | | | | |
| 80 | 10 | 1 | 1 | 3 | | | | | | | | | | | | | | | | | | | | | | | | | | | | | | | | | | |
| 81 | 17 | 1 | 3 | 2 | 3 | | | | | | | | | | | | | | | | | | | | | | | | | | | | | | | | | |
| 82 | 38 | 0 | 0 | 2 | 3 | 3 | 2 | 3 | 3 | 1 | | | | | | | | | | | | | | | | | | | | | | | | | | | | |
| 83 | 16 | 0 | 1 | 2 | 3 | 1 | | | | | | | | | | | | | | | | | | | | | | | | | | | | | | | | |
| 84 | 25 | 1 | 3 | 3 | 3 | 2 | 1 | | | | | | | | | | | | | | | | | | | | | | | | | | | | | | | |
| 85 | 25 | 0 | 2 | 3 | 2 | 3 | 3 | 1 | | | | | | | | | | | | | | | | | | | | | | | | | | | | | | |
| 86 | 18 | 1 | 2 | 3 | 3 | 2 | | | | | | | | | | | | | | | | | | | | | | | | | | | | | | | | |
| 87 | 24 | 3 | 3 | 2 | 3 | 1 | 0 | | | | | | | | | | | | | | | | | | | | | | | | | | | | | | | |
| 88 | 21 | 1 | 2 | 3 | 1 | | | | | | | | | | | | | | | | | | | | | | | | | | | | | | | | | |
| 89 | 24 | 3 | 3 | 3 | 2 | | | | | | | | | | | | | | | | | | | | | | | | | | | | | | | | | |
| 90 | 19 | 1 | 2 | 3 | 2 | | | | | | | | | | | | | | | | | | | | | | | | | | | | | | | | | |
| 91 | 15 | 2 | 3 | 3 | | | | | | | | | | | | | | | | | | | | | | | | | | | | | | | | | | |
| 92 | 29 | 1 | 2 | 3 | 3 | 1 | 0 | | | | | | | | | | | | | | | | | | | | | | | | | | | | | | | |
| 93 | 30 | 1 | 2 | 3 | 3 | 2 | 1 | | | | | | | | | | | | | | | | | | | | | | | | | | | | | | | |
| 94 | 13 | 3 | 3 | 2 | | | | | | | | | | | | | | | | | | | | | | | | | | | | | | | | | | |
| 95 | 21 | 3 | 3 | 2 | 2 | 1 | 0 | | | | | | | | | | | | | | | | | | | | | | | | | | | | | | | |
| 96 | 26 | 2 | 3 | 1 | 3 | 2 | | | | | | | | | | | | | | | | | | | | | | | | | | | | | | | | |
| 97 | 12 | 1 | 3 | 1 | | | | | | | | | | | | | | | | | | | | | | | | | | | | | | | | | | |
| 98 | 20 | 1 | 3 | 2 | 1 | | | | | | | | | | | | | | | | | | | | | | | | | | | | | | | | | |
| 99 | 16 | 2 | 3 | 2 | 0 | | | | | | | | | | | | | | | | | | | | | | | | | | | | | | | | | |
| 100 | 41 | 0 | 1 | 0 | 2 | 3 | 3 | 3 | 2 | 1 | 0 | 2 | 0 | | | | | | | | | | | | | | | | | | | | | | | | | |
| 101 | 12 | 1 | 2 | 3 | 2 | 2 | | | | | | | | | | | | | | | | | | | | | | | | | | | | | | | | |
| 102 | 13 | 3 | 3 | 1 | | | | | | | | | | | | | | | | | | | | | | | | | | | | | | | | | | |
| 103 | 24 | 2 | 2 | 3 | 2 | 2 | | | | | | | | | | | | | | | | | | | | | | | | | | | | | | | | |
| 104 | 14 | 0 | 1 | 3 | 2 | 1 | | | | | | | | | | | | | | | | | | | | | | | | | | | | | | | | |

F/EF3 Catalogs

| | | | | | | | | | | | | | | | | | | | | | | | | | | | | | | | | | | | |
|-----|------|---|---|---|---|---|---|---|---|---|---|---|---|---|---|---|---|---|---|---|---|---|---|---|---|---|---|---|---|---|---|---|---|---|---|
| 105 | 17 | 2 | | | | 3 | | | | 2 | | | | 1 | | | | | | | | | | | | | | | | | | | | | |
| 106 | 35 | 1 | | 2 | | 1 | | 3 | | 2 | | 3 | | 2 | | 1 | | | | | | | | | | | | | | | | | | | |
| 107 | 12 | 0 | | | | | | | | 3 | | | | | | | | | | | | | | | | | | | | | | | | | |
| 108 | 9 | 2 | | | | 3 | | | | 2 | | | | | | | | | | | | | | | | | | | | | | | | | |
| 109 | 4 | 1 | | 2 | | 3 | | 2 | | 0 | | | | | | | | | | | | | | | | | | | | | | | | | |
| 110 | 27 | 0 | 0 | 0 | 0 | 1 | 1 | 2 | 2 | 3 | 3 | 2 | 1 | 1 | 2 | 1 | 0 | 0 | 1 | 0 | 0 | 0 | | | | | | | | | | | | | |
| 111 | 5 | 1 | | | | 2 | | | | 3 | | | | | | | | | | | | | | | | | | | | | | | | | |
| 112 | 3.5 | 3 | | | | 2 | | | | | | | | | | | | | | | | | | | | | | | | | | | | | |
| 113 | 24.5 | 2 | | 1 | | 2 | | 1 | | 3 | | 3 | | 1 | | 2 | | 1 | | 2 | | 2 | | 1 | | 1 | | 1 | | | | | | | |
| 114 | 5.8 | 1 | | | | 3 | | | | 2 | | | | 1 | | | | 1 | | | | | | | | | | | | | | | | | |
| 115 | 14 | 1 | | 1 | | 0 | | 0 | | 1 | | 0 | | 2 | | 0 | | 0 | | 3 | | 1 | | 1 | | 2 | | 0 | | 1 | | 1 | | 0 | |
| 116 | 10 | 0 | | 1 | | 2 | | 2 | | 2 | | 2 | | 3 | | 2 | | 1 | | 0 | | | | | | | | | | | | | | | |
| 117 | 121 | 2 | 4 | 2 | 1 | 0 | 2 | 2 | 3 | 4 | 4 | 3 | 2 | 1 | 0 | 2 | 2 | 4 | 3 | 2 | 2 | 2 | 2 | 3 | 0 | 1 | 2 | 0 | 4 | 1 | | | | | |
| 118 | 20 | 3 | | | | 4 | | | | 2 | | | | 1 | | | | | | | | | | | | | | | | | | | | | |
| 119 | 22 | 1 | | 2 | | 3 | | 4 | | 2 | | 0 | | 0 | | | | | | | | | | | | | | | | | | | | | |
| 120 | 37 | 0 | | 1 | | 2 | | 3 | | 3 | | 4 | | 2 | | | | | | | | | | | | | | | | | | | | | |
| 121 | 38 | 2 | | 3 | | 3 | | 3 | | 4 | | 4 | | 3 | | 2 | | | | | | | | | | | | | | | | | | | |
| 122 | 28 | 0 | | 1 | | 4 | | 4 | | 2 | | 1 | | 0 | | | | | | | | | | | | | | | | | | | | | |
| 123 | 20 | 0 | | 2 | | 3 | | 4 | | 1 | | 1 | | | | | | | | | | | | | | | | | | | | | | | |
| 124 | 21 | 2 | | 4 | | 3 | | 2 | | 1 | | | | | | | | | | | | | | | | | | | | | | | | | |
| 125 | 28 | 0 | | 4 | | 0 | | 1 | | 0 | | | | | | | | | | | | | | | | | | | | | | | | | |
| 126 | 42 | 2 | | 3 | | 4 | | 3 | | 4 | | 3 | | 2 | | 1 | | 1 | | | | | | | | | | | | | | | | | |
| 127 | 36 | 0 | | 1 | | 4 | | 3 | | 2 | | 2 | | 2 | | 0 | | | | | | | | | | | | | | | | | | | |
| 128 | 29 | 2 | | 3 | | 4 | | 4 | | 4 | | 3 | | 2 | | | | | | | | | | | | | | | | | | | | | |
| 129 | 35 | 0 | | 4 | | 4 | | 4 | | 3 | | 3 | | 1 | | | | | | | | | | | | | | | | | | | | | |
| 130 | 30 | 1 | | 1 | | 2 | | 3 | | 4 | | 4 | | 3 | | | | | | | | | | | | | | | | | | | | | |
| 131 | 26 | 2 | | 3 | | 4 | | 3 | | 2 | | 2 | | | | | | | | | | | | | | | | | | | | | | | |
| 132 | 19 | 4 | | 4 | | 2 | | 2 | | 2 | | 1 | | | | | | | | | | | | | | | | | | | | | | | |
| 133 | 32 | 0 | | 4 | | 4 | | 3 | | 0 | | 2 | | 1 | | 0 | | | | | | | | | | | | | | | | | | | |
| 134 | 13 | 0 | | 2 | | 3 | | 4 | | 4 | | 4 | | | | | | | | | | | | | | | | | | | | | | | |
| 135 | 36 | 3 | | 4 | | 4 | | 3 | | 2 | | 1 | | 0 | | | | | | | | | | | | | | | | | | | | | |
| 136 | 50 | 3 | | 3 | | 4 | | 4 | | 4 | | 4 | | 4 | | 3 | | 2 | | 0 | | | | | | | | | | | | | | | |
| 137 | 103 | 0 | 1 | 1 | 1 | 1 | 2 | 1 | 2 | 3 | 4 | 2 | 2 | 2 | 2 | 1 | 1 | 2 | 0 | 2 | 1 | | | | | | | | | | | | | | |
| 138 | 26 | 0 | | 1 | | 2 | | 4 | | 3 | | 2 | | | | | | | | | | | | | | | | | | | | | | | |
| 139 | 22 | 3 | | 3 | | 4 | | 3 | | 3 | | 3 | | | | | | | | | | | | | | | | | | | | | | | |
| 140 | 24 | 2 | | 4 | | 3 | | 2 | | | | | | | | | | | | | | | | | | | | | | | | | | | |
| 141 | 39 | 0 | 1 | 2 | 2 | 2 | 2 | 2 | 3 | 4 | 3 | 4 | 3 | 2 | 2 | 2 | 2 | 1 | 1 | 2 | 2 | 2 | 1 | 2 | 1 | 0 | | | | | | | | | |
| 142 | 47 | 0 | 1 | 1 | 2 | 3 | 4 | 4 | 3 | 3 | 4 | 3 | 3 | 4 | 3 | 3 | 2 | 1 | 0 | 0 | 0 | 1 | 1 | 2 | 2 | 2 | 1 | 1 | 2 | 2 | 1 | 0 | | | |
| 143 | 10 | 1 | | 3 | | 4 | | 4 | | 2 | | 0 | | | | | | | | | | | | | | | | | | | | | | | |
| 144 | 13 | 0 | | 0 | | 1 | | 3 | | 1 | | 1 | | 2 | | 1 | | 2 | | 4 | | 1 | | 1 | | | | | | | | | | | |
| 145 | 52 | 0 | 1 | 1 | 1 | 0 | 0 | 1 | 1 | 1 | 0 | 1 | 0 | 0 | 1 | 2 | 4 | 2 | 4 | 4 | 4 | 2 | 1 | 2 | 2 | 3 | 4 | 2 | 2 | 1 | 2 | 3 | 1 | 0 | 0 |
| 146 | 32 | 3 | | 5 | | 4 | | 2 | | 2 | | 0 | | | | | | | | | | | | | | | | | | | | | | | |
| 147 | 62 | 0 | | 0 | | 1 | | 2 | | 3 | | 4 | | 5 | | 4 | | 4 | | 3 | | 4 | | 4 | | 2 | | | | | | | | | |
| 148 | 21 | 0 | | 1 | | 2 | | 5 | | 3 | | | | | | | | | | | | | | | | | | | | | | | | | |
| 149 | 34 | 1 | | 3 | | 3 | | 4 | | 5 | | 5 | | 4 | | 1 | | | | | | | | | | | | | | | | | | | |
| 150 | 51 | 1 | | 3 | | 4 | | 3 | | 3 | | 5 | | 5 | | 4 | | 4 | | | | | | | | | | | | | | | | | |
| 151 | 102 | 0 | 0 | 0 | 1 | 2 | 5 | 5 | 3 | 3 | 3 | 3 | 2 | 3 | 2 | 2 | 3 | 2 | 3 | 2 | 3 | 2 | 0 | 1 | | | | | | | | | | | |
| 152 | 37 | 1 | 1 | 2 | 3 | 3 | 4 | 4 | 3 | 4 | 5 | 5 | 4 | 4 | 4 | 4 | 2 | 3 | 4 | 5 | 4 | 4 | 3 | 4 | 4 | 4 | 4 | 2 | | | | | | | |
| 153 | 35 | 5 | | | | 5 | | | | 4 | | | | 2 | | | | | | | | | | | | | | | | | | | | | |
| 154 | 43.5 | 5 | | | | 5 | | | | 2 | | | | 2 | | | | 2 | | | | | | | | | | | | | | | | | |
| 155 | 31 | 0 | 1 | 2 | 3 | 3 | 4 | 5 | 4 | 5 | 4 | 3 | 3 | 2 | 2 | 2 | 2 | 3 | 2 | 3 | 2 | 3 | 2 | 3 | 2 | 1 | 1 | 1 | 1 | 0 | | | | | |

7. SUMMARY AND CONCLUSIONS

Intensity variation during a tornado's life cycle is an important input to tornado wind speed risk assessment. Tornado wind speed risk for individual buildings is linearly related to the intensity conditional probabilities, $P(I_i^*|F/EF)$. These probabilities represent a mean fraction summary of the local path length intensity ratings, conditional on the tornado maximum F/EF rating.

Damage-based maximum intensity estimates along tornado path lengths provide an important source of data for the quantification of PLIV. In particular, tornadoes that have been evaluated systematically with F/EF scale ratings along their entire path length provide a unique source of information. Tornadoes that have only been rated on one small portion of the length or have radar data for only a portion of the life cycle are not a source of data for PLIV. Such data is useful for shorter time period (and path length) changes in intensity vs. the full path length and longer averaging times and path lengths used herein.

Damage-based PLIV analysis is limited because it is dependent on DI density and location along the tornado path. Damage maps in rural areas are more likely to have missed the maximum tornado intensity due to a lower likelihood of the tornado coming in contact with a DI. In addition, some DIs are wind speed-limited in the maximum intensity rating they can obtain (e.g. a barn can be rated a maximum of EF2), and this fact also confounds the inference of PLIV from damage data. In addition, there are many uncertainties in F/EF scale assignments, as noted by Twisdale et al. (2016). PLIV analysis based on F/EF ratings is therefore subject to considerable uncertainties and potential biases. The results herein are clearly subject to all of these limitations.

We performed PLIV analyses for two sources of data: NGR and GR. The NGR data includes PLIV data from 155 \geq F/EF1 tornadoes. Aerial surveys were incorporated for many of the tornadoes comprising the NGR data. The GR data includes data from 550 \geq F/EF1 tornadoes from the DAT database for the years 2010-2014.

The NGR data are based on tornado damage maps, such as those created by Fujita (1975), Speheger et al. (2002), and others. The average rating spacing of all the NGR data was 3.7 miles. Hence, the tornado intensity is assumed to be constant over this length. The average number of segments for F/EF1-F/EF5 was 2.6, 4.5, 5.8, 10.5, and 12.5, respectively. The NGR results show that F/EF1 through F/E5 tornadoes sustain their maximum

F/EF intensities over 62, 48, 36, 25, and 23% of their respective path lengths, on average. These values constitute the principal diagonal of the $P(I_i^*|F/EF)$ developed PLIV matrix. The full matrix of mean values, standard deviations, coefficients of variations, minimums, and maximums are given in Table 7.

The GR PLIV analysis was based on DAT EF scale data. The analysis of the DAT data was complicated by many factors and required the use of statistical regression of the data coupled with a kernel length analysis to develop intensity variation data in a usable form. The results were highly dependent on the kernel length. Short kernel lengths produced much smaller principal diagonal fractions. They also produced very high EF0 fractions for all intensities and other inconsistencies. When we used a 4 mile kernel length, the principal diagonal fraction results were very similar to the NGR data. The results for the 4 mile (persistence) kernel provided reasonable confirmation of the NGR data, which is mostly composed of F scale rating data.

Given the current state of available PLIV data, we believe that the best sources of data are NGR maps where the intensity ratings are given for consistent segment lengths along the entire tornado path. The developed PLIV model has an inherent assumption of tornado intensity persistence over a distance of about 4 miles. Variations of intensity over shorter distances and associated time periods cannot be treated with the method used herein.

We found that the PLIV fractions within each F/EF scale were well fit by a linear function. Therefore, we smoothed this data by fitting linear models to the $P(I_i^*|F/EF)$ distributions. The smoothing removed small non-linearities in the data and the final results are given in Table 7.

PLIV can be modeled in tornado risk assessment using the mean fraction tables developed herein or through the catalogue of 155 \geq F/EF1 tornadoes given in Table 8. The catalogue approach is useful for modeling tornado risk for large spatially-distributed systems, such as transmission lines, groups of facilities, and insurance portfolios. A Markov process approach could also be used to model intensity state changes along the tornado path length, using the data in Table 8.

An interesting result of the NGR PLIV analysis was the computed mean tornado intensity over the full path length of tornadoes. We found that the mean intensity was 0.44, 1.04, 1.73, 2.09, and 2.85 for EF1 through EF5, respectively. The mean path length intensity is therefore about a 0.6, 1, 1.3, 2, and 2.1 intensity drop from the tornado maximum rating for EF1 through EF5.

This analysis showed that the mean intensity decreased with increasing path length for all F/EF scales. However, the amount of variance explained by path length was small for the moderate and intense tornadoes (F/EF 2-5, as illustrated in Figure 3b).

Another insight from the PLIV analysis is that the maximum intensity typically occurs near the center of the path. This observation is consistent with the generally recognized tornado life cycle characteristics of a formation stage, mature stage, and dissipation stage. We found that the maximum intensity damage rating was observed 45, 90, and 52% of the time within each sequential one third of the normalized path length, with similar trends observed when broken out by F/EF-Scale. In addition, we counted the number of events that had a unimodal maximum rating type of damage-based life cycle and 85% had this characteristic.

Due to the importance of PLIV in tornado wind speed risk assessment, we encourage more studies of tornado life cycle intensity variation. Long period radar observations could provide direct data on intensity variations at both macro and micro scale levels. Numerical windfield modeling, with consideration of roughness effects may also provide clues on intensity variations. Super-cell and non-super-cell tornadoes are likely to have different time scales of intensity variation, and separate PLIV models could be used based on storm type. Detailed damage surveys, together with aerial photography, are likely to provide the best source of data for the foreseeable future. Systematic path length intensity variation analysis using the DAT toolkit could also provide a good source of data, particularly when coupled with both ground and aerial surveys.

8. ACKNOWLEDGMENTS

This work is funded by the National Institute of Standards and Technology (NIST) under the "Tornado Risk Maps for Building Design" project (SB1431-12-CQ-0014). Special thanks are given to Dr. Long Phan (NIST) and Dr. March Levitan (NIST) for their inputs and feedback regarding this work. Applied Research Associates (ARA) is acknowledged for providing partial funding for the preparation of this conference paper and the associated conference poster.

9. REFERENCES

Atkins, N. T., Butler, K. M., Flynn, K. R., & Wakimoto, R. M. (2014). An Integrated Damage, Visual, and Radar Analysis of the 2013 Moore, Oklahoma, EF5 Tornado. *Bulletin of the American Meteorological Society*, 95(10), 1549-1561.

Burgess, D. W., Magsug, M. A., Wurman, J., Dowell, D. C., and Richardson, Y., (2002). Radar Observations of

the 3 May 1999 Oklahoma City Tornado. *Weather and Forecasting*, Vol. 7.

Forbes, G. S. (1978). The Cabot, Arkansas Tornado of March 29, 1978, *Satellite & Mesometeorology Research Project*, 167, Department of the Geophysical Sciences, the University of Chicago.

Fujita, T. T. (1975). Super Outbreak of tornadoes of April 3-4, 1974. Map printed by University of Chicago Press.

Fujita, T. T. (1978). Aerial Survey of Grand Gulf Plant and Vicinity after the April 17, 1978 Tornado. *Satellite & Mesometeorology Research Project*, 162, Department of the Geophysical Sciences, the University of Chicago.

Fujita, T. T., and Wakimoto, Roger M. (1979). Red River Valley Tornado Outbreak of April 10, 1979. Map printed by the University of Chicago.

Grazulis, T. P., (2001). *The Tornado: Nature's Ultimate Windstorm*. University of Oklahoma Press.

Kosiba, K., Wurman, J., Richardson, Y., Markowski, P., Robinson, P., and Marquis, J., (2013). Genesis of the Goshen County, Wyoming, Tornado on 5 June 2009 during VORTEX2. *Monthly Weather Review*, Vol. 141.

Marshall, T. P., Davies, W., and Runnels, S. (2012). Damage Survey of the Joplin Tornado: 22 May 2011. *26th Conference on Severe Local Storms*, Nashville, TN.

Marshall, T. P., McCarthy, D., LaDue, J. G., Wurman, J., Alexander, C. R., Robinson, P., and Kosiba, K. A. (2008a). Damage Survey of the Greensburg, KS Tornado. *24th Conference on Severe Local Storms*, Savannah, GA.

Marshall, T. P., Jungbluth, K., and Baca, A. (2008b). The Parkersburg, IA Tornado: 25 May 2008. *24th Conference on Severe Local Storms*, Savannah, GA.

NOAA (2016). NWS Damage Assessment Toolkit. <https://apps.dat.noaa.gov/StormDamage/DamageViewer/>

NWS Norman, (1998). The Moore, Oklahoma Tornado of 4 October 1998. Map. NWS NOAA. 7 Dec. 2016. <https://www.weather.gov/oun/events-19981004-mooretornado>

NWS Omaha/Valley & Emergency Management, (2004). Hallam, NE Tornado May 22, 2004. Map. NWS NOAA. <http://w2.weather.gov/images/oax/Archives/hallam/hallammap.jpg>

NWS Omaha/Valley, (2008). Little Sioux Scout Ranch Tornado, June 11, 2008. Map. NWS NOAA. <http://w2.weather.gov/oax/LittleSioux>

- NWS Sioux Falls, (1992). Chandler-Lake Wilson Minnesota F5 Tornado of June 16, 1992. Map. NWS NOAA. 7 Dec. 2016. <http://www.weather.gov/fsd/19920616-tornado-chandlerlakewilson>
- NWS Sioux Falls, (2003). 24 June 2003 Tornado Tracks. Map. NWS NOAA. 7 Dec. 2016. <http://www.weather.gov/fsd/20030624-tornadotracks>
- NWS Sioux Falls, (2004). Tornado Tracks over Clay County Iowa on June 11, 2004. Map. NWS NOAA. <http://www.weather.gov/fsd/20040611-tornado-claycounty>
- NWS Sioux Falls, (2006). Maps of the Beadle County Tornado Paths – August 24, 2006. Map. NWS NOAA. http://www.weather.gov/fsd/tor2006aug24_path
- Reinhold, T. A. and Ellingwood, B., (1982). Tornado Damage Risk Assessment. NUREG/CR-2944; BNL-NUREG-51586. National Bureau of Standards, Washington, DC. Center for Building Technology.
- Speheger, D. A., Doswell, C. A., III, and Stumpf, G. J., (2002). The Tornadoes of 3 May 1999: Event Verification in Central Oklahoma and Related Issues. *Weather and Forecasting*, 17, 362-381.
- Twisdale, L.A., Dunn, W. L., Horie, Y., and Davis, T.L. (1981). Tornado Missile Simulation and Design Methodology, Volume 2: Model Verification and Data Base Updates. *Electric Power Research Institute NP-2005*, Vol. 2.
- Twisdale, L. A., Dunn, W. L., Lew, S. T., Davis, T. L., Hsu, J. C., and Lee, S. T., (1978). Tornado Missile Risk Analysis, Electric Power Research Institute, EPRI NP-768 and NP-769 (Appendixes), Palo, Alto, CA, May.
- Twisdale, L. A., (1978), "Tornado Data Characterization and Windspeed Risk," *Journal of the Structural Division*, ASCE, Vol. 104, No. ST10, October.
- Twisdale, L. A., Banik, S. S., Vickery, P. J., Levitan, M., Phan, L., (2016). A Methodology for Improving Tornado Damage-Based Intensity Ratings. 28th Conference on Severe Local Storms, Portland, OR.
- Wakimoto, R., Murphey, H. V., Dowell, D. C., and Bluestein, H. B. (2003). The Kellerville Tornado during VORTEX: Damage Survey and Doppler Radar Analyses. *Monthly Weather Review*, 131, 2197-2221.
- Wakimoto, R. M. and Wilson, J. W. (1989). Non-supercell Tornadoes. *Monthly Weather Review*, 117, 1113-1140.
- Ramsdell, J. V. and Rishel, J. P., (2007). Tornado Climatology of the Contiguous United States. *Nuclear Regulatory Commission Report*. NUREG/CR-4461, Rev. 2; PNNL-15112, Rev. 1.
- Smith, B. and Adams, B., (2004). Walnut, IA Tornado May 8, 2004. Map. NWS NOAA. 7 Dec. 2016. http://w2.weather.gov/images/oax/Archives/walnut_tor/s-canmap.jpg
- Smith, B. and Zapotocny, C., (2003). Coleridge, NE Tornado, June 23, 2003. Map. NWS NOAA. 7 Dec. 2016. <http://w2.weather.gov/oax/coleridge>
- Wakimoto, R. M., Atkins, N. T., Wurman, J., (2011). The LaGrange Tornado During VORTEX2. Part I: Photogrammetric Analysis of the Tornado Combined with Single-Doppler Radar Data. *Monthly Weather Review*, 139, 2233-2258.